Effect of Gyrus Folding Angle on Peak Electric Field in Cerebral Cortex

Lorette Quéguiner, Gabriel Gaugain, Julien Modolo, Denys Nikolayev

Effect of gyrus folding angle on peak electric field in cerebral cortex

Lorette Quéguiner (/user/9978) [1], Gabriel Gaugain (/user/9939) [1], Julien Modolo (/user/1337) [2] & Denys Nikolayev (/user/6735) [1]

[1]*IETR (Institut d'Électronique et des Technologies du numéRique) UMR 6164, CNRS, Rennes, France, 35000*
[2]*LTSI (Laboratoire de Traitement du Signal et de l'Image) U1099, INSERM, Rennes, France, 35000*
BioEM2021, Ghent, Belgium, Sep 26 - 30, 2021 *(/node/37973)*

Keywords: Dosimetry (computational), All Frequencies, Completed (unpublished)
Presented by: Lorette Quéguiner

Reported transcranial current stimulation (tCS) effects on cerebral activity leave numerous questions open regarding the involved mechanisms of action. A number of studies have identified clear physiological effects, however it remains to be understood how to take into account interindividual variability to tCS: For example, to what extent does individual brain geometry, such as cerebral tissues morphology, impact this prediction? Here, we aimed at evaluating how the geometry of cortical tissue surfaces impacts the charge distribution and therefore the electric fields induced by tCS.

Introduction

Non-invasive brain stimulation (NIBS) is gaining increasing interest in neuroscience. Indeed, countless studies have suggested therapeutic potential in the field of drug-refractory depression [Boggio et al., 2008], Parkinson's disease [Lee et al., 2019], and stroke [Fregni et al., 2005], among others. NIBS can be induced using at least two electrodes that cause a transcranial current flow, which can be either alternative (tACS) or direct (tDCS). Effects of tCS on cerebral activity depend directly on the electric field generated in brain tissues [Bikson et al., 2004; Radman et al., 2009; Rahman et al., 2013].

Since the brain shape is non-deterministic, personalized therapy is laborious and expensive, requiring individual magnetic resonance imaging (MRI) to tailor and predict the therapeutic effect. The distribution of E-field in heterogeneous brain tissues varies indeed significantly as a function of individual shape and size [Truong et al., 2013; Laakso et al., 2015]. Moreover, the electric field in any disordered heterogeneous media will exhibit local maxima and minima in vicinity of convex and concave features and, in particular, close to wedge-shaped gyri as a direct consequence of Gauss's law. The goal of this study was therefore to quantify the influence of cortical gyri shape on the distribution of the local electric field.

Methods

The MRI data used in this study was from the ICBM model: an averaged geometry of a large number of healthy human brains [Fonov et al., 2011]. In order to build a numerical model based on this geometry, our first step was the segmentation of tissues using the ROAST pipeline [Huang et al., 2018]. Then, an axial slice was chosen to accurately represent the cross-sectional anatomy of the brain. The resulting slice is presented in Figure 1, and consists of the raw MRI data (Figure 1a) and the segmented representation (Figure 1b). The segmented slice was then outlined using the Inkscape vector editing software. As shown in Figure 1c, Bezier curves were defined for the boundary of each tissue to obtain a complete vector image suitable for finite element modeling in COMSOL Multiphysics.

The dielectric parameters were attributed according to the Cole–Cole model [Gabriel et al., 1996]. At 1 kHz, the following tissue properties were defined as: skin [$\sigma = 2.0 \times 10^{-4}$ (S/m); $\varepsilon_r = 1.1 \times 10^3$]; scalp [$\sigma = 2.0 \times 10^{-2}$ (S/m); $\varepsilon_r = 2.7 \times 10^3$]; cerebrospinal fluid [CSF; $\sigma = 2.0$ (S/m); $\varepsilon_r = 1.1 \times 10^2$]; grey matter [GM; $\sigma = 9.0 \times 10^{-2}$ (S/m); $\varepsilon_r = 1.6 \times 10^5$]; white matter [WM; $\sigma = 6.0 \times 10^{-2}$ (S/m); $\varepsilon_r = 7.0 \times 10^4$]; where σ is the conductivity and ε_r is the relative permittivity. The conductive gel for electrodes was modelled by two rectangles intersecting with the surface of the skin (Figure 1d). The insulator boundary condition ($J \cdot n = 0$) was assigned to the skin surface. The outer boundaries of gel modelled the electrodes with $V = 0$ for the ground and $I_0 = 2$ mA for the terminal (Figure 1d).

The next step was to isolate a gyrus close to electrodes where a wedge angle can be varied with a minimal E-field disturbance from surrounding tissues. For the variation of the angle, three control points (A, B, C) were defined (Figure 2b). (B, C) remained fixed while A was moved to adjust the angle (Figure 2b). The degree of this angle θ can be evaluated from the coordinates of (A, B, C) by calculating their Euclidian distance. For this, we used Al-Kashi's theorem

$$\theta_N = cos^{-1} \frac{d(A,C)^2 + d(A,B)^2 - d(B,C)^2}{2 \times d(A,C) \times d(A,B)}$$

where d(X, Y) denotes the Euclidian distance between the two points X and Y. Ten angles $\theta_n \in [68.1, 143.7]$ were established, as shown in Figure 2b. Normalized electric field was evaluated on the wedge point A.

Results and Discussion

Figure 2a highlights a non-homogeneous distribution of the electric field along the interfaces between tissues. As hypothesized, these variations were more pronounced at the interfaces with locally strong convex or concave features.

Figure 2c presents the local E-field distribution on a gyrus as a function of the wedge angle. Clearly, the E-field amplitude on the CSF–GM decays exponentially as a function of the wedge angle (Figure 3). This dependence can be accurately interpolated as $E = 0.5933\ e^{-0.017\theta}$ (coefficient of determination $R^2 = 0.9986$), where E is the E field and θ is the wedge angle. The effect of the wedge angle was significant: locally, the electric field doubled for an angle from 143° to 68°. Importantly, this variation in amplitude can affect the focality of neurostimulation in cortical regions.

Conclusion

This study did show the significant influence of gyri shape, especially its wedge angle, on the local distribution of E-field in the cerebrospinal fluid. More than an observation, it is actually an exponential dependence that was identified. Those results emphasize the importance of taking into account subject-specific brain morphology, which could explain at least in part the lack of consistency between numerous tCS studies. Having improved estimates of electric field distributions in target regions could also assist in calibrating stimulation intensities to facilitate the comparison of outcomes between subjects.

Acknowledgment

This study was supported in part by the LabEx CominLabs "PKSTIM" and in part by the French region of Brittany through the SAD "EM-NEURO."

References

Bikson M, Inoue M, Akiyama H, Deans JK, Fox JE, Miyakawa H, Jefferys JGR. 2004. Effects of uniform extracellular DC electric fields on excitability in rat hippocampal slices in vitro: Modulation of neuronal function by electric fields. The Journal of Physiology 557:175–190.

Boggio PS, Rigonatti SP, Ribeiro RB, Myczkowski ML, Nitsche MA, Pascual-Leone A, Fregni F. 2008. A randomized, double-blind clinical trial on the efficacy of cortical direct current stimulation for the treatment of major depression. Int J Neuropsychopharmacol 11:249–254.

Fonov V, Evans AC, Botteron K, Almli CR, McKinstry RC, Collins DL, Brain Development Cooperative Group. 2011. Unbiased average age-appropriate atlases for pediatric studies. Neuroimage 54:313–327.

Fregni F, Boggio PS, Mansur CG, Wagner T, Ferreira MJL, Lima MC, Rigonatti SP, Marcolin MA, Freedman SD, Nitsche MA, Pascual-Leone A. 2005. Transcranial direct current stimulation of the unaffected hemisphere in stroke patients. Neuroreport 16:1551–1555.

Huang Y, Datta A, Bikson M, Parra LC. 2018. ROAST: An open-source, fully-automated, realistic volumetric-approach-based simulator for TES. Annu Int Conf IEEE Eng Med Biol Soc 2018:3072–3075.

Laakso I, Tanaka S, Koyama S, De Santis V, Hirata A. 2015. Inter-subject variability in electric fields of motor cortical tDCS. Brain Stimul 8:906–913.

Lee HK, Ahn SJ, Shin YM, Kang N, Cauraugh JH. 2019. Does transcranial direct current stimulation improve functional locomotion in people with Parkinson's disease? A systematic review and meta-analysis. J Neuroeng Rehabil 16:84.

Radman T, Ramos RL, Brumberg JC, Bikson M. 2009. Role of cortical cell type and morphology in subthreshold and suprathreshold uniform electric field stimulation in vitro. Brain Stimulation 2:215-228.e3.

Rahman A, Reato D, Arlotti M, Gasca F, Datta A, Parra LC, Bikson M. 2013. Cellular effects of acute direct current stimulation: somatic and synaptic terminal effects. J Physiol 591:2563–2578.

Truong DQ, Magerowski G, Blackburn GL, Bikson M, Alonso-Alonso M. 2013. Computational modeling of transcranial direct current stimulation (tDCS) in obesity: Impact of head fat and dose guidelines. NeuroImage: Clinical 2:759–766.

Figures

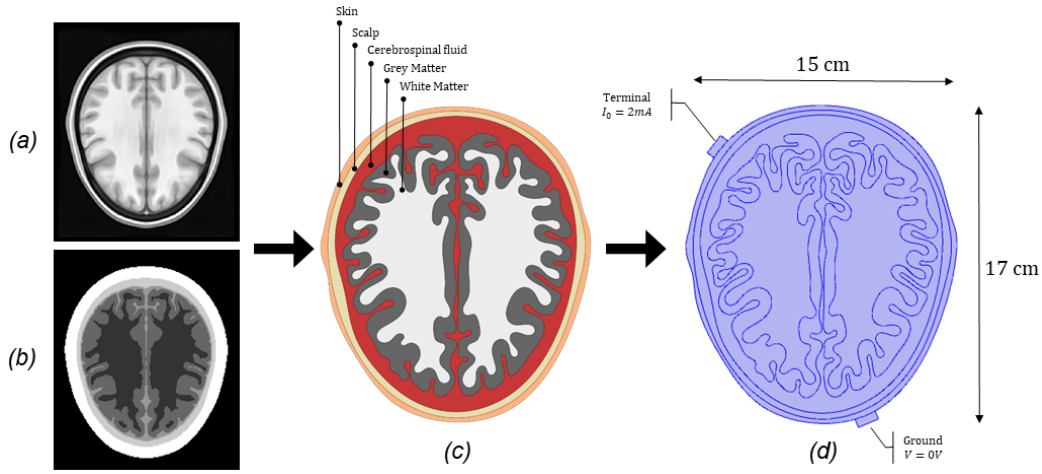

Figure 1. Model formulation using a 2D cerebral axial slice (a) Source image from ICBM model (105 out of 189 images); (b) ROAST classification; (c) Phantom obtained with vectorization of tissues; (d) Final model including gel and electrodes.

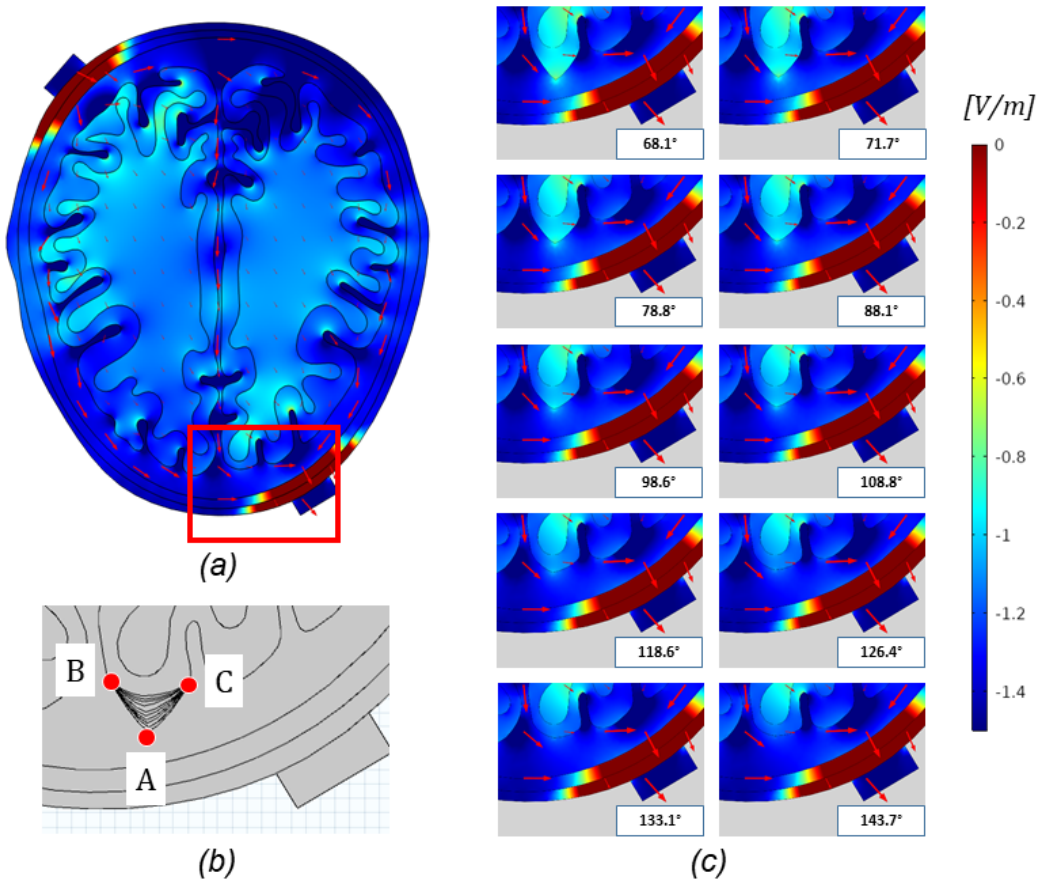

Figure 2. (a) Electric field distribution on the global surface with an input current of 2mA at 1 kHz; (b) Variation of the wedge angle θ from 68° to 143°; and (c) Associated electric field distribution.

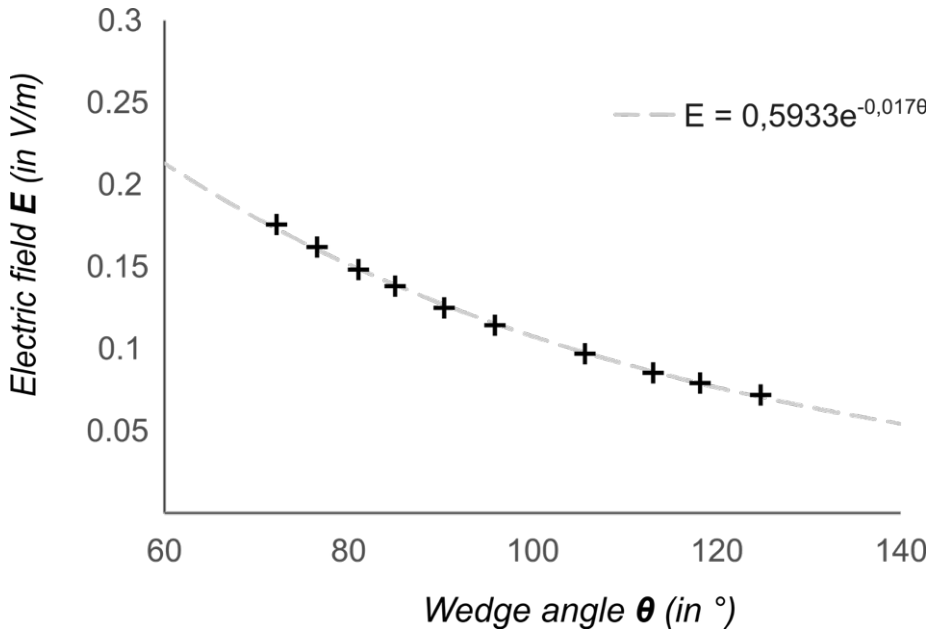

Figure 3. Effect of the wedge angle on the maximum electric field.